

Computational Modelling of T Cell Receptor Interaction Geometry

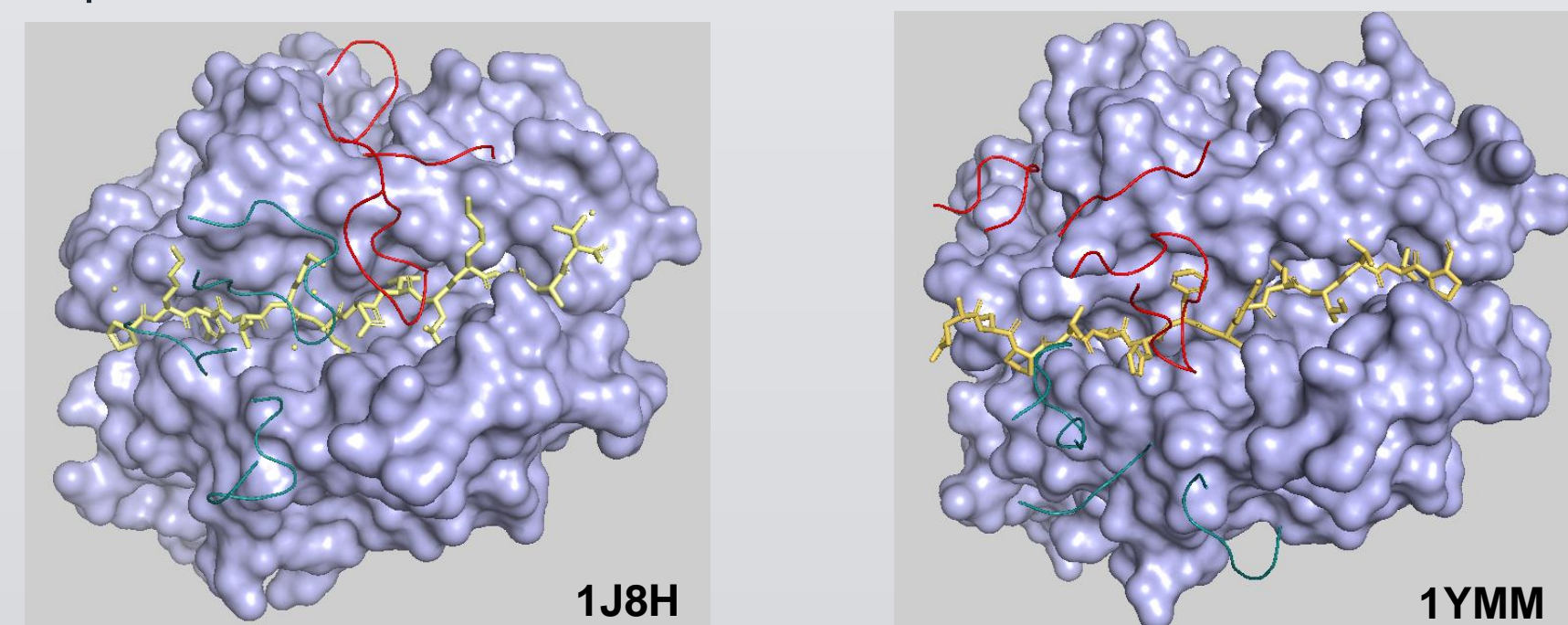
Stephanie DeVoe and Shaodong Dai, PhD

University of Colorado Anschutz



Introduction

How a T cell receptor (TCR) recognizes its antigen greatly affects the quality of signal and level activation received by the T cell, subsequently dictating the following immune response. Regions in the TCR known as complementary determining regions (CDRs) are the structural components that contact the surface of the peptide-major histocompatibility complex (pMHC) and confer specificity to the TCR. Each chain of the TCR, alpha (TRA) and beta (TRB), has 3 CDRs. CDRs1+2 are germline encoded and usually maintain contact with the MHC helices. CDR3 is unique from V(D)J recombination and usually maintains the majority of the contact with the peptide antigen. When interacting with a foreign antigen (ie non-self), TCRs typically orient diagonally across the pMHC surface across the center of the peptide. In atypical cases, such as structure 1YMM – an autoreactive TCR to myelin basic protein, the orientation of the TCR is shifted to the N-terminus of the peptide and is more orthogonal to the pMHC surface.



Left: Structure 1J8H – TCR HA1.7 and influenza HA-HLA-DR4. **Right:** Structure 1YMM – a HLA-DR2 restricted, autoimmune TCR specific for myelin basic protein. CDRa's are displayed as teal ribbon structures. CDRb's are displayed as red ribbon structures. Peptides are displayed as yellow licorice structures. HLA molecules are displayed as light blue surface representations.

Conventionally, the docking angle of a TCR has been defined by the cross-product of the vector formed from the linear fit of the MHC binding groove and the vector formed from the centroids of conserved disulfide bonds in TRA and TRB chains. However, this fails to account for the most critical aspects of TCR-pMHC interactions: the CDRs.

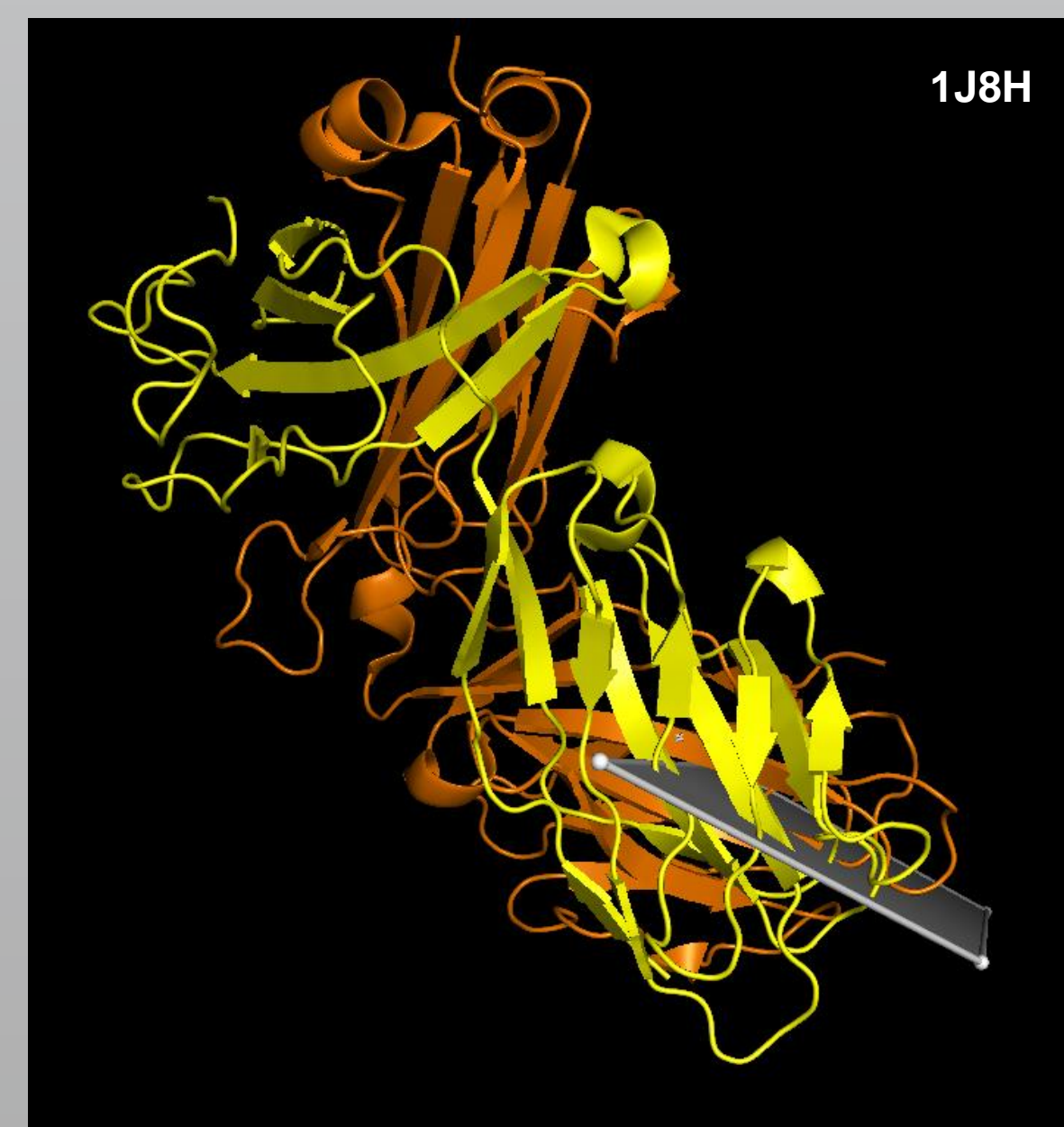
Objectives

Expand upon the conventional docking angle to better characterize TCR-pMHC interaction geometry by modelling a:

- TCR plane using all atoms of the CDRs
- TCR plane using only the TCR residues that have contact with the pMHC surface
- TRA plane
- TRB plane
- TCR germline plane using only atoms of CDRs1+2
- TRA germline plane
- TRB germline plane

Determine the impact of CDR3 on TCR orientation

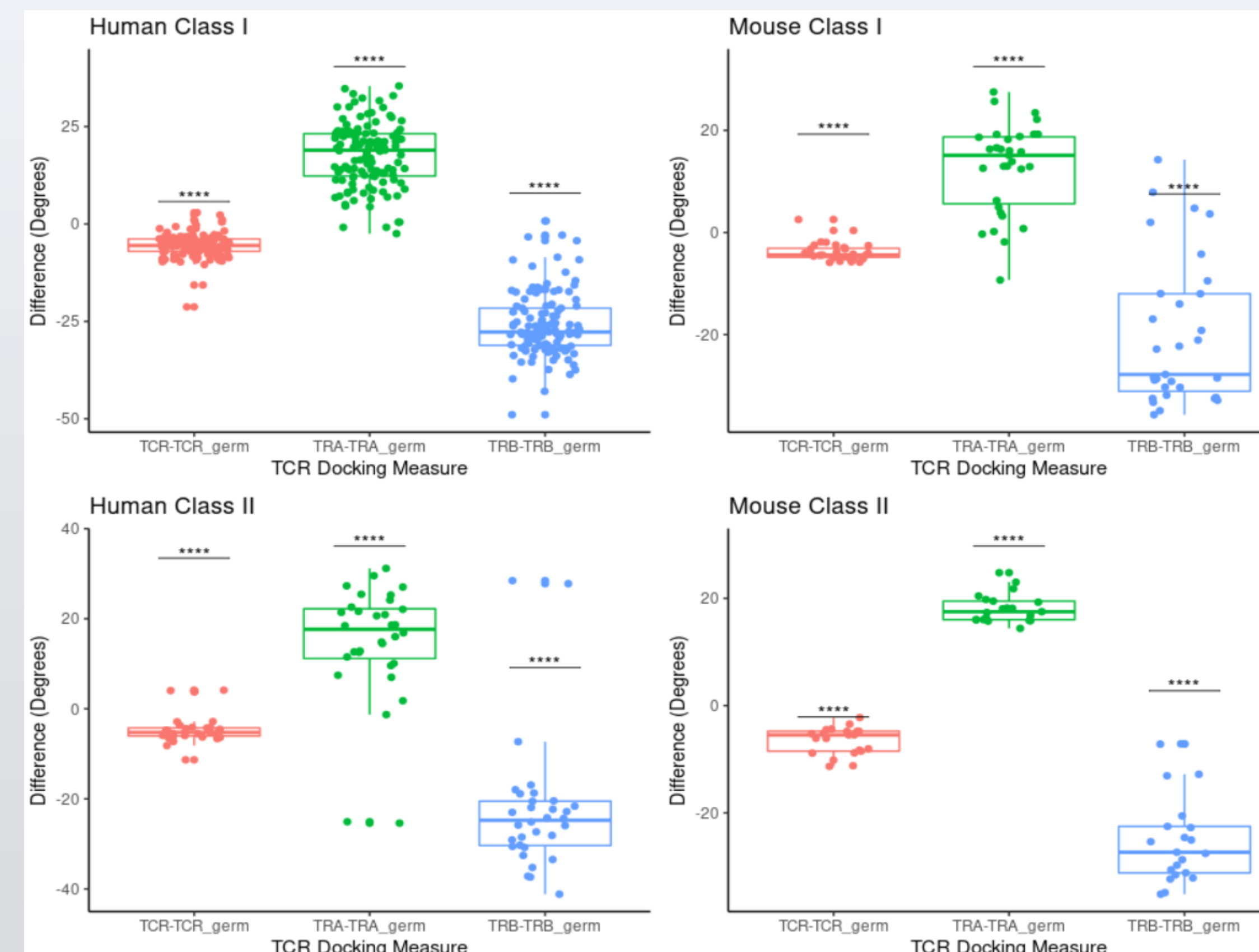
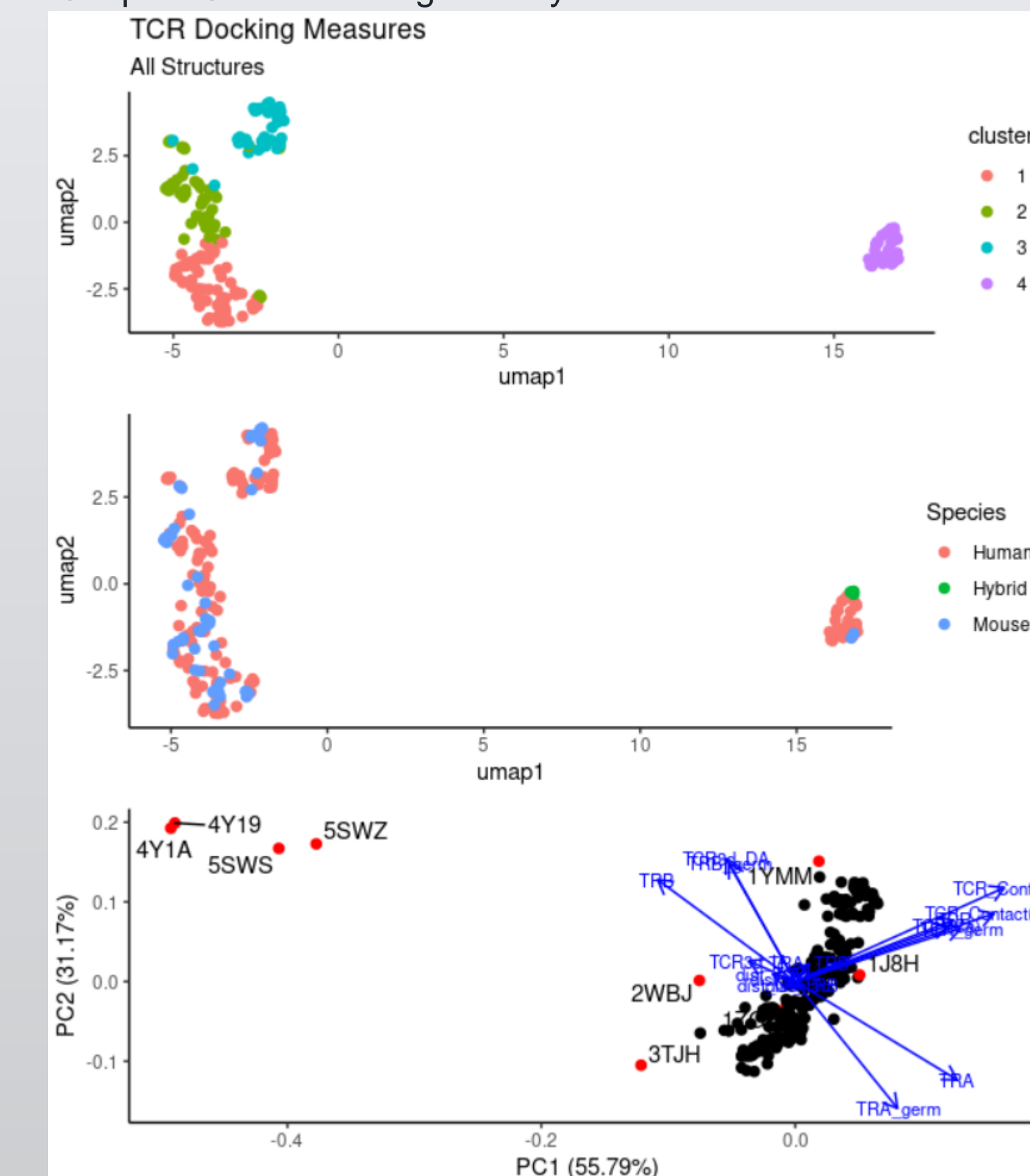
Compare germline interactions of well-studied TRBV-containing TCRs



The TCR of structure 1J8H overlaid with its TCR plane model. **Yellow** = TRA chain. **Orange** = TRB chain

Results

TCR characterization based on expanded docking angle model (below). Angles between each plane parameter and the binding groove of 213 TCR-pMHC structures were determined. Of these structures 31 were murine class I, 21 were murine class II, 4 were alloreactive murine TCRs against human HLA, 125 were human class I, and 32 were human class II. UMAP dimensionality reduction and unsupervised cluster identification by nearest neighbors community detection algorithms determined 4 clusters exist among the known mouse and human TCR-pMHC structures based on our expansion of the characterization of TCR-pMHC interaction geometry.



Influence of CDR3 on TCR-pMHC interaction geometry (above). Differences in human class I structures were found to be a median of -5.53° for TCR, 18.94° for TRA, and -27.72° for TRB between the respective germline models. Differences in human class II structures were found to be a median of -5.23° for TCR, 17.66° for TRA, and -24.74° for TRB between the respective germline models. Differences in mouse class I structures were found to be a median of -4.41° for TCR, 15.11° for TRA, and -27.81° for TRB between the respective germline models. Differences in mouse class II structures were found to be a median of -5.58° for TCR, 17.50° for TRA, and -27.34° for TRB between the respective germline models. **Orange:** difference in angle of TRA plane to the binding groove and TRA germline plane to the binding groove. **Green:** difference in angle of TRB plane to the binding groove and TRB germline plane to the binding groove. **Blue:** difference in angle of TCR plane to the binding groove and TCR germline plane to the binding groove. **** denotes a p-value < 10⁻⁵

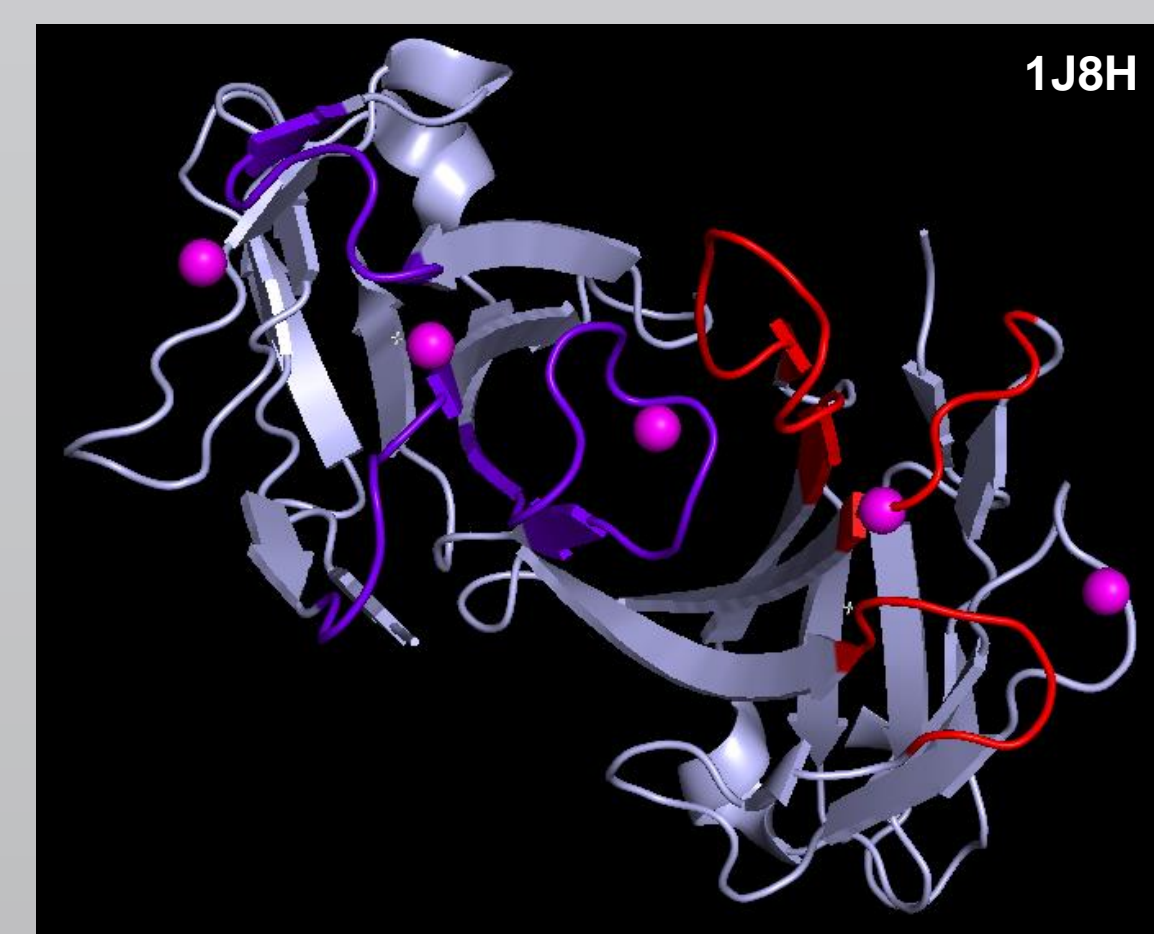
Methods

Plane Modelling

A python script was created to retrieve the PDB file of structure from RCSB.org, determine the equation of the binding groove of the MHC, and model the planes of TCR components. A linear regression of the Ca atoms of the helices forming the binding groove in the MHC was used to determine the binding groove vector. A line and point were used to generate the normal vector defining each plane of the TCR. The equation of the line used to determine the plane was determined from a linear regression fit of the specified atom coordinates from the PDB file of the structure. The point used to determine the plane was the center of mass of the V(D)J region of the TCR component.

TCR component	Line points	Center of Mass Region
TCR	all CDR atoms	TRA and TRB V(D)J
TCR contact	TCR atoms within 5 Angstroms of pMHC surface	TRA and TRB V(D)J
TRA	CDRa atoms	TRA VJ
TRB	CDRb atoms	TRB VDJ
TCR germline	CDRs1+2 atoms	TRA and TRB V(D)J
TRA germline	CDR1a and CDR2a atoms	TRA VJ
TRB germline	CDR1b and CDR2b atoms	TRB VDJ

Directionality was defined from N to C terminus for the binding groove vector. For the TCR component planes, directionality was defined by the cross-product from the Alpha chain direction to the Beta chain direction. For the TRA and TRB planes, this equates to the cross-product from the CDR2 direction to the CDR1 direction.



V(D)J region of the TCR of structure 1J8H. View from the CDRs towards the constant region (Above). View from the side of the TCR (below). **Pink spheres** = Linear regression vector of the CDRs of structure 1J8H. **Purple** = CDRa's. **Red** = CDRb's. **Teal** = TCR V(D)J center of mass



Angle Calculations

The angle between the normal vector of a plane and a line is defined as follows:

$$\cos \theta = \frac{m \cdot n}{|m||n|}$$

where θ is the angle between the normal vector of the plane (m) and the line (n)

The angle between a plane and a line is the complement of the angle between the normal vector of the plane and the line. Therefore, when we let the angle between a plane and a line be represented by ϕ :

$$90^\circ - \theta = \phi$$

$$\cos \theta = \sin(90^\circ - \theta)$$

$$\cos \theta = \sin \phi$$

$$\cos \theta = \frac{m \cdot n}{|m||n|} = \sin \phi$$

$$\phi = \sin^{-1} \frac{m \cdot n}{|m||n|}$$

This method will result in angles ranging from -90° to 90°, where 0° is parallel and negative angles indicate a reversed direction.

Statistical Analysis

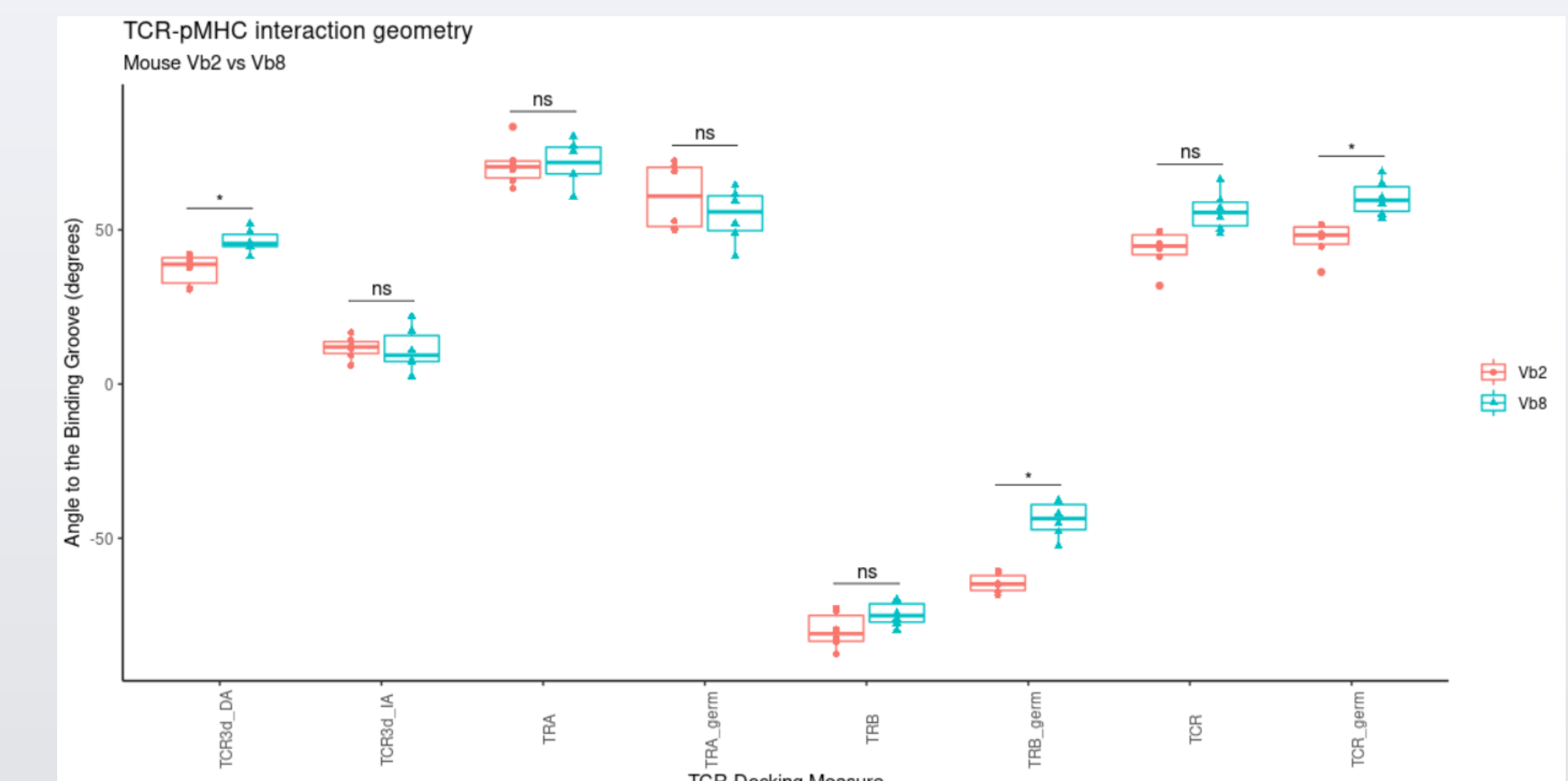
Dimension reduction was performed with UMAP in R using the package uwot and nearest neighbor clustering was performed with the package bluster. Differences between TCR Docking Measures and germline interactions were calculated in R using Mann-Whitney U testing with Bonferroni multiple testing corrections.

Software

Pymol version 2.4.0a0; Python version 3.8.2

R version 4.0.3; bluster version 1.0.0; uwot version 0.1.9

Results



Murine TCRs containing Vb2 and Vb8 are among the most well-studied TCR structures. The median conventional docking angle (TCR3d_DA) for Vb2 is 38.85° and for Vb8 is 45.55°. The median TRB germline (TRB_germ) docking angle for Vb2 is -64.86° and for Vb8 is -43.61°. The median TCR germline (TCR_germ) docking angle for Vb2 is 48.31° and for Vb8 is 59.58°. Vb2 structure PDB IDs: 1FO0, 1KJ2, 1NAM, 2OL3, 6X31, and 6DFS. Vb8 structure PDB IDs: 4N5E, 3RDT, 3C6L, 3C5Z, 3RGV, and 6DFW. * denotes a p-value < 0.05 and ns denotes not significant

Conclusions

TCR-pMHC interaction geometry is defined by set rules and restrictions that govern which orientations a TCR may take as suggested by the strict clustering in the UMAP plot. The dispersion of mouse and human structures in each cluster also suggests mouse and human TCRs follow the same set of rules and restrictions for pMHC recognition. Principle component analysis also shows the ability of the expanded model to detect TCRs with flipped orientations: 4Y19, 4Y1A, 5WSW, and 5SWZ.

CDR3 alters the interaction geometry of each chain and the TCR as a whole to the pMHC surface. The TCR undergoes a 4.5 to 5.5 degree decrease, where the angle to the binding groove becomes more parallel. The TRA chain undergoes a 15 to 19 degree increase, where the angle to the binding groove becomes less parallel. The TRB chain undergoes a 24 to 27 decrease, where the angle to the binding groove becomes less parallel.

Differences in the conventional docking angle of the murine Vb2 and Vb8 TCR suggests that Vb2 approaches the pMHC surface at a less steep angle than Vb8. However, expanding upon the conventional method reveals that the difference in the orientation of the two chains can be attributed to the germline contacts where Vb2 actually approaches the pMHC surface at a more steep angle than Vb8.

Future Research

Determine common features of TCRs within the same cluster. We hypothesize TCRs will cluster by MHC restriction and type of antigen (eg self, viral, bacterial, etc). If common cluster features can be defined, we plan to adapt this model as a predictive function for TCRs screened by library where the true antigen is unknown.

TCRs for NKT and MAIT cells which recognize non-traditional MHC molecules, CD1 and MR1 respectively, will also have their interaction geometry analyzed to determine how the orientation compares between T cells, NKT cells, and MAIT cells.

Reference angles will be established to determine the areas of contact by each CDR in varying TCR orientations. A focus will be on the extent of CDR contact with each MHC helix and the peptide antigen in differing angles.

References

1. Beringer, D. X., et al. (2015). "T cell receptor reversed polarity recognition of a self-antigen major histocompatibility complex." *Nature Immunology* 16(11): 1153-1161.
2. Dai, S., et al. (2008). "Crossreactive T Cells Spotlight the Germline Rules for 㬑㬢 T Cell- Receptor Interactions with MHC Molecules." *Immunity* 28(3): 324-334.
3. Gowthaman, R. and B. G. Pierce (2019). "TCR3d: The T cell receptor structural repertoire database." *Bioinformatics* 35(24): 5323-5325.
4. Gras, S., et al. (2016). "Reversed T Cell Receptor Docking on a Major-Histocompatibility Class I Complex Limits Involvement in the Immune Response." *Immunity* 45(4): 749-760.
5. Hahn, M., et al. (2005). "Unconventional topology of self peptide-major histocompatibility complex binding by a human autoimmune T cell receptor." *Nature Immunology* 6(5): 490-496.
6. Harkiolaki, M., et al. (2009). "T Cell-Mediated Autoimmune Disease Due to Low-Affinity Crossreactivity to Common Microbial Peptides." *Immunity* 30(3): 348-357.
7. Hennecke, J. and D. C. Wiley (2002). "Structure of a Complex of the Human αβ T Cell Receptor (TCR) HA1.7, Influenza Hemagglutinin Peptide, and Major Histocompatibility Complex Class II Molecule, HLA-DR4 (DRA*0101 and DRB1*0401): Insight into TCR Cross-Restriction and Alloreactivity." *Journal of Experimental Medicine* 195(5): 571-581.
8. Rudolph, M. G., et al. (2006). "HOW TCRS BIND MHCs, PEPTIDES, AND CORECEPTORS." *Annual Review of Immunology* 24(1): 419-466.
9. Scott-Brown, James P., et al. (2011). "Evolutionarily Conserved Features Contribute to 㬑㬢 T Cell Receptor Specificity." *Immunity* 35(4): 526-535.